Comparative study of *Cladophora* sp. cellulose by using FTIR and XRD

Comparative study of *Cladophora* sp. cellulose by using FTIR and XRD

S W Suciyati[1, 2], P Manurung[2], S Sembiring[2], R Situmeang[3]

[1]Ph.D Student, Doctoral Program of Mathematics and Natural Science, Faculty of Mathematics and Natural Sciences, University of Lampung, Jl. Sumantri Brojonegoro no 1, Bandar Lampung, Indonesia
[2]Department of Physics, Faculty of Mathematics and Natural Sciences, University of Lampung, Jl. Sumantri Brojonegoro no 1, Bandar Lampung, Indonesia
[3]Department of Chemical, Faculty of Mathematics and Natural Sciences, University of Lampung, Jl. Sumantri Brojonegoro no 1, Bandar Lampung, Indonesia

E-mail: sri.wahyu@fmipa.unila.ac.id

Abstract. Cellulose Crystalline *Cladophora* sp. (CCC) was successfully isolated from the freshwater algae *Cladophora* sp. by used the hydrolysis method. The alkaline treatment can affect the structure of CCC that is showed by the spectrum of Fourier Transform Infrared (FTIR). The typical range for lignin does not appear here, which indicates the delignification process using NaOH plus hydrolysis of HCl has succeeded in removing lignin. The spectrum associated with functional group impurity (1800-1050 cm^{-1}) with lipid, protein, and nucleid acid content are still seen after alkaline treatment and acid hydrolysis. Analysis of crystallinity with X-ray Diffraction (XRD) data showed that CCC had the highest crystallinity index on CD-K (93.4%), Cd-P (66.6%), and Cd-S (63.04%). The smallest particle size for each cellulose is Cd-K (9.5 nm), Cd-S (25.23 nm), and Cd-P (49.57 nm). Based on these results, the CCC production from *Cladophora* sp. using alkaline and acid hydrolysis treatment is enough to get samples with high crystallinity. The CCC product has the potential to be an excellent reinforcing material for biomaterial-based polymer materials.

1. Introduction

Cellulose considered an organic compound that biosynthesized from a number of living organisms, such as higher plants, algae, bacteria, fungi, and sea animals (tunicate). The chemical structure of cellulose $(C_6H_{10}O_5)_n$ represents more than 50% carbon content in it. The chemical structure of cellulose consists of repeating units of β-1,4-linked anhydro-D-glucose, which are linked together through oxygen, covalently binds to C1 from one glucose ring to C4 from the adjacent ring (1-4 linkage) and is called a β,1–4 glucosidic bond [1]. The basic structural component of cellulose formed during biosynthesis is called microfibrils. In fibrils, there are regions with very regular layers (crystalline cellulose) and random layers (amorphous cellulose). The part of crystal in cellulose is commonly isolated for various cellulose-based biomaterial applications due to its characteristic stiffness, low density, flexibility, large aspect ratio, and unique rheology, which is mostly due to the crystal assembly through hydrogen bonds [2][3][4]. Hydrogen bonds in hydroxyl functional groups on the surface can interact electrostatically in binding applications related to adhesion between micro/nanoparticles cellulose and other materials [5], for example, in hybrid composites [6] and paper

production [7], environment and water-related areas [8] [9], biomedical applications [10] [11], and energy storage devices [6][12][13] [14].

The structure of cellulose is forming by hydrogen bonds between the network of hydroxyl groups [15][16]. Structural analysis and functional group characteristics methods are essential for the development of cellulose applications related to synthetic reaction procedures and cellulose-based counterfeit products. The cellulose crystal structure is known by X-ray diffraction using a monoclinic cell unit consisting of two cellulose chains in a parallel orientation and two folding screw axes [17]. In the cellulose crystal structure, there are four main polymorphs (I, II, III, IV) with most natural cellulose being cellulose I (cellulose crystals). Cellulose I has two polymorphs, namely Iα (triclinic structure) and Iβ (monoclinic structure), with different amounts in cellulose depending on the source of cellulose [18]. Iα structure dominates polymorphs from algae and bacterial, while Iβ dominates polymorphs from higher plants and tunicates. The characteristics of the chemical composition and functional groups of cellulose can be determined by FTIR spectroscopy, which measures the intensity and wavelength of absorption of infrared radiation (IR) by samples [19][20]. The typical wavelength range for applications is 4000-400 cm^{-1}, ie the absorption band region with the transition between vibrational energy state and substrate rotation of molecule. Functional group analysis is divided into several spectra which indicate the presence of stretching vibrations OH of α-cellulose, lignin, absorption of water by cellulose, C-O-C stretching of β-1,4-glycosidic bonds and C-H cellulose vibrations related to β-glycosidic linkage [19] [21-30]. The presence of stretching and vibration in OH functional groups has the advantage of forming cellulose composites with synthetic polymers and biopolymers or the formation of cellulose-based hybrid materials [6][31][32]. The ability of OH groups to form hydrogen bonds has an essential role in the formation of fibrilar and semicrystalline packaging, which controls the physical features of highly cohesive cellulose material [33].

Cellulose could extract from lignocellulosic biomass such as from wood, plants, bacteria, and algae using various methods to obtain pure micro- or nano-sized cellulose [34][35][18][36][37]. Lignocellulosic biomass contains cellulose, hemicellulose, and lignin. The appropriate treatment is needed to remove matrix material (hemicellulose and lignin) and isolate fibers. Extraction methods include mechanical, chemical, or enzymatic methods that can apply at the preparation and extraction stages of cellulose crystal structures. The preparation stage generally uses chemical methods such as alkali and bleaching, which aim to remove lignin, hemicellulose, wax, and oil, which cover the outer surface of the cell wall of fiber [38]. Crystalline cellulose extraction is doing by breaking the amorphous phase through chemical, mechanical, or enzymatic methods [39][40][41]. Several studies have isolated the crystalline phase using acid hydrolysis [24][29][42], mechanical treatment [43], and enzymatic hydrolysis [2][43] individually or by combining these methods. Acid hydrolysis methods combined with microfluidization or ultrasound treatments after alkaline pretreatment have commonly used to obtain micro/nanocrystalline cellulose because of their simplicity and low energy consumption. In contrast, mechanical methods involve high energy consumption, which can cause dramatic reductions in yield and length of fibrils if used separately, so they are often combining with chemical methods or enzymatic methods [44]. The enzymatic method is usually using after partial hydrolysis with acids or bases before continuing mechanical techniques (e.g., grinding, microfluidizing, or ultrasonication) [24].

The purpose of this study is to examine the functional group of cellulose from freshwater algae sources, *Cladophora* sp., which has extracted using acid hydrolysis and alkali-bleaching pretreatment methods. Crystal cellulose powder obtained was characterized using FTIR and XRD for a more detailed investigation of functional groups and their crystallinity. An understanding of the fundamental properties of these functional groups (hydroxyl groups) is crucial regarding the most reactive hydroxyl groups so that chemical modification of cellulose can apply for better application.

2. Materials and methods

Fresh green algae samples, *Cladophora* sp., were obtained from three places, namely the former rice fields, trenches, and small ponds for fish. Each sample is called *Cladophora* sp. Sawah (Cd-S), *Cladophora* sp. Trench (Cd-P), and *Cladophora* sp. Pool (Cd-K). The samples then cleaned of dirt, plants, and water animals that stick by washing the sample in running water then dried in the sun to dry.

Materials chemicals such that $NaClO_2$ (Pharmaceutical Grade, Merck), NaOH (Pharmaceutical Grade, Bratachem), HCl (Pharmaceutical Grade, Bratachem), distillate water, and glacial acetic acid (Merck) used for cellulose synthesis. Algae samples were prepared by washing, drying, and mashing using a blender and then sieved with a 60 mesh. The extraction process generally develops procedures [34], namely bleaching-alkali pretreatment and acid hydrolysis. The initial procedure is the treatment of delignification and purification, then the acid hydrolysis process to obtain cellulose crystals.

The sample bleached with a sodium acetate buffer solution for 3 hours in a water bath (60 ^{0}C). The solid part is separated and washed with DI water to neutral using a centrifuge at 4000 rpm for 10 minutes. After six washing, the solid is mixed with 0.5 M NaOH and heated in a water bath (60 ^{0}C) overnight, then washed with DI water using a centrifuge and dried. After drying, the sample is mixed with 5% HCl and heated (~ 90 ^{0}C) to boiling and then cooled to room temperature overnight. The sample washed to neutral, dried, mashed, and sieved with a 200 mesh sieve.

Characterization of the samples carried out using FTIR Cary 630 Agilent brand. FTIR is a non-destructive technique for determining biomass components in the mid-IR spectrum. Samples characterized by spectra recorded in the range 650-4000 cm^{-1} for 32 scans. FTIR describes the chemical structure by identifying functional groups in the sample and the intensity of the infrared absorption band. X-ray diffraction (XRD) measurements performed by XRD type PANanalytical: X'Pert Pro diffraction analyzer. The diffracted intensity of Cu K-alpha radiation (k = 1.54056 A˚) at 40 kV and 40 mA was measuring in a 2θ range of 5°–90°. The Segal crystallinity index (CI) calculated by using the following equation [24],

$$CI = \frac{I_{\max} - I_{\min}}{I_{\max}} x100\% \quad (1)$$

where I_{max} is the intensity of the highest peak, I_{min} is the minimum intensity at a 2θ close to 18° for cellulose I. The particle size of cellulose (L) is calculated by the Scherrer equation:

$$l = \frac{K\lambda}{B\cos\theta} \quad (2)$$

where K is a form correction factor (0,9), λ is the wavelength of the radiation (1.541874 Å), B is FWHM from the highest diffraction peak (rad), and θ is half of the diffraction angle.

3. Results and discussion

3.1 Cellulose powder from different material sources

Dissolving cellulose sources in alkalis such as NaOH [45] [46] [47] [48] [49] can produce cellulose with a percentage of purity depending on the concentration of NaOH given. While the bleaching treatment with $NaClO_2$ ensures complete removal of lignin until the sample is lighter in color. Figure 1 shows three algae samples from *Cladophora* sp. taken from three different locations before and after being extracted.

The source of cellulose material has a different color depending on the environment, where Cd-P has a darker tone compared to Cd-K and Cd-S. This difference has also seen in the cellulose powder produced. Alkali-bleaching pretreatment and acid hydrolysis treatment have been carrying out on

algae *Cladophora* sp., and cellulose powder products obtained. The alkali-bleaching process does not fully brighten the color of Cd-P powder, which indicates the presence of impurity content in Cd-P cellulose.

Figure 1. Raw (above) and powder (down) materials for (a) Cd-S, (b) Cd-P, and (c) Cd-K

3.2 FTIR

FTIR characterized powder samples and the spectrum has shown in Figure 2. Analysis of functional groups and infrared signal spectrum (IR) with the possibility of existing compounds refer to the report [26] [28] [50][51]. The analysis has performed in two wavenumber regions, namely 3700-2800 cm^{-1} and 1650-600 cm^{-1}. In general, the biomass component mostly contains alkene, esters, aromatics, ketones, and alcohol compounds, where the IR absorbance of the -OH and C-O groups is highest in cellulose. The C=O bonding compound is dominant in hemicellulose, while lignin is associated with skeletal aromatic vibrations found in the fingerprint region (1860-790 cm^{-1}) [28].

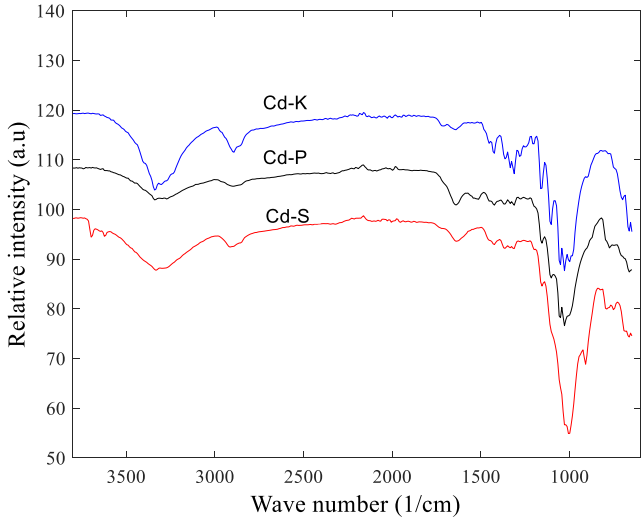

Figure 2. The FTIR spectra of celluloses powder from *Cladophora* sp.

3.2.1 Range spectra FTIR 3700-2800 cm^{-1}

This range spectra is characteristic for stretching vibration of OH and C-H bonds in polysaccharides. Figure 2 with the peak widened at 3332 cm^{-1} (Cd-S), 3340 cm^{-1} (Cd-P) and 3340 cm^{-1} (Cd-K) related to stretching vibration of OH groups in polysaccharides, including the vibrations of inter- and intra-molecular bonds in cellulose from the CH_2-OH structure [24][26][50][51]. Shifting and widening peaks (Cd-P and Cd-S) indicate a weak hydroxyl bond in the OH group in cellulose, making it possible to modify Cd-P and Cd-S cellulose into biocomposite material. Peaks at 2914 cm^{-1} (Cd-S), 2890 cm^{-1} (Cd-P) and 2892 cm^{-1} (Cd-K) is formed due to vibration stretching and bending C-H on all hydrocarbons [24] so it cannot be used as a benchmark because all alkanes contain this functional group (peaks 2920-2800 cm^{-1}). The functional groups characteristics in Figure 2, correspond to the cellulose FTIR results extracted from *Cladophora* glomerata [24].

3.2.2 Range spectra FTIR 1650–600 cm^{-1}

This range of spectra is a typical band for cellulose, generally expressing the existence of bending bonds CH_2 and -CH, –OH and C-O, and vibrations of water molecules. From Figure 2, the peak of 1640 cm^{-1} corresponds to the vibrations of water molecules absorbed by cellulose, and this peak owned by all cellulose *Cladophora* sp. The peak of 1543 cm^{-1} in Cd-P cellulose attributed to stretching C=O from ketone and carbonyil compounds [28]. This peak is considered a characteristic of lignin [52]. The range of wavenumber 1520-1400 cm^{-1} shows the widening of the peak in cellulose due to the functional groups bending CH_2, C-H and C-O which attributed to the aromatic skeletal ring [50] [51], especially for the peak of 1423 cm^{-1} (Cd-S cellulose) associated with bending vibrations of $–CH_2$ bonds. The spectrum associated with functional group impurity is characterizing by the presence of such proteins, according to [53] detected in the range 1600-1500 cm^{-1}, according to [20] the presence of impurity functional groups such as lipids, proteins, and nucleid acids are in the range 1800-1050 cm^{-1}. The distribution of these peaks is of low intensity, so that Cd-S, Cd-P, and Cd-K cellulose has a small amount of protein, lipid, and nucleid acid. Figure 2 shows that Cd-K cellulose contains the most functional group impurity, especially in the range of 1520-1200 cm^{-1}. Impurity with low absorption intensity has also seen in Cd-S, and Cd-P cellulose, which means that lipid, protein, and nucleid acid content is also present in these celluloses in small amounts. The peak at 1423 cm^{-1} is also associated with the amorph [51] of the cellulose crystal structure, which indicates that the amorph region cannot be removed entirely by the alkaline-acid hydrolysis process. The absorption band at 1600-1500 cm^{-1} according to [26] shows the presence of lignin, where in Cd-P cellulose there is an absorption peak (1513 cm^{-1}) which indicates the presence of lignin despite the alkaline treatment. This is also shown by the color of Cd-P powder which is not completely bright compared to Cd-S and Cd-K.

The wavenumber range 1300-1200 cm^{-1} in Cd-K is associated with the impurity of functional groups (nucleid acid) [20] by stretching C-O-C from aryl-alkyl ether compounds [26]. Range wavenumber 1110-900 cm^{-1} shows OH functional groups associated with C-OH and C-H bending from aromatic hydrogen compounds. These peaks overlap with the lignin component [26], so that in Cd-S and Cd-P are estimated that the delignification process with the alkaline treatment has partially removed the lignin. The spectrum associated with functional group impurity has also detected in the range of intensity of wavenumber 1110-1050 cm^{-1} [20] with lipid, protein, and nucleid content. The intensity of IR absorption at the peak of 790-690 cm^{-1} indicates the stretching of C-C and stretching C-H from aromatic hydrogen compounds. The peak of 790 cm^{-1}, 775 cm^{-1}, 782 cm$^{-1,}$ according to [51] is an amorphic structure in Cd-S, Cd-P, and Cd-K cellulose.

Characteristics of FTIR absorption bands for algae *Cladophora* sp. have been summarized in Table 1, showing the suitability of the results with some previous studies [24][54].

Table 1. Spectra characteristics of FTIR *Cladophora* sp. cellulose, Commercial microcrystalline cellulose (CMCC) and data reported

Assignment	Wavenumber (cm^{-1})					
	Cd-S	Cd-P	Cd-K	CMCC(1)*	(1)*	(2)*
-OH groups stretching vibration	3332	3340	3340	3347	3420	3340
C-H stretching vibration	2914	2899	2892	2895	2897	2900
H_2O absorbed	1640	1640	1640	1633	1632	-
CH_2 bending vibration	1423	1423	1423	1428	1430	1429
C-O-C glycosidic band stretching vibration	1028	1028	1028	1162	1164	1060
C-H rock vibration	909	-	998	897	898	893

(1)* : [54]
(2)* : [24]

3.3 XRD

An X-ray diffractometer has used to analyze the crystallinity of cellulose powder. The cellulose powders from Cd-S, Cd-P, and Cd-K were analyzed and shown in Figure **3**. The spectrum produced by the XRD diffraction analyzer uses a step size 0.017, X-rays radiation source: Cu-Kα with a wavelength of 1.541874 Å.

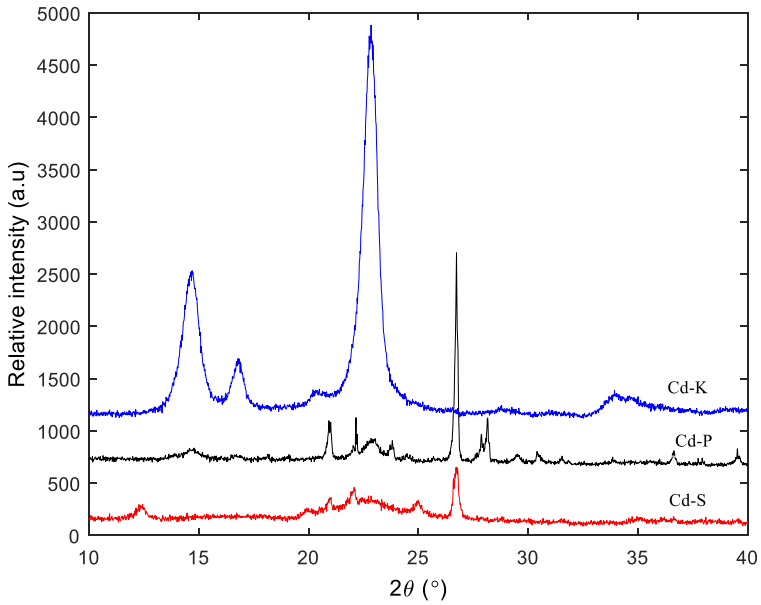

Figure 3. XRD patterns of cellulose at ambient temperature for Cd-K, Cd-P and Cd-S. Wavelength = 1.541874 Å

Figure 3 shows that all powder samples have revealed the peaks of diffraction at certain 2θ. This indicated that powder samples prepared by hydrolysis have contained crystal besides amorphous phases. All patterns had peaks at 22.86° as the indication of cellulose phase eventhough the highest peak occurred only Cd-K. Generally all samples indicate high crystallinity as shown the peaks 14.7, 16.79, and 22.86°. The peaks observed at 2θ = 20.1° (Cd-K) and 22° (Cd-P and Cd-S) showed allomorphic coexistence of cellulose I and cellulose II [52]. A possible explanation is related to the re-precipitation of cellulose after acid hydrolysis treatment, where a hydrochloric acid solution might be

a solvent for cellulose. The crystallinity index was calculated based on equation (1) and particle size of cellulose was counted by equation (2) and the results are presented in Table 2.

Table 2. The particle size and crystalinity of *Cladophora* sp.

CMC/CNC sources	FWHM (°)	Partikel size (nm)	Crystallinity (%)
Cd-K	0.831	9.5	93.4
Cd-S	0.317	25.23	63.04
Cd-P	0.164	49.57	66.6

As comparison, the particle size of Cd-K of 9.5 nm is very close to Xiang, *et al* [24] that cellulose produced from *Cladophora* glomerata algae. Based on particle size of nanomaterial (1-100 nm), the cellulose of this research has the particle size relatively low. It indicates that a procedure series in preparing cellulose powder is match to the expectation.

4. Conclusions

Cellulose Crystalline *Cladophora* sp. (CCC) was successfully isolated from the freshwater algae *Cladophora* sp., which was taken from three different locations. The results of the FTIR analysis confirmed that the chemical structure of the cellulose fragments was affected by alkaline treatment and acid hydrolysis. This influence is seen in the peaks of infrared absorption, which are assumed to be a component of lignin; the intensity decreases. Analysis of the XRD pattern of CCC showed that CD-K cellulose has a very crystalline structure with a particle size of 9.5 nm, better than Cd-P and Cd-S. Based on these results, it can be concluded that the CCC production from *Cladophora* sp. using alkaline treatments and acid hydrolysis is enough to get samples with high crystallinity. The CCC product has the potential to be an excellent reinforcing material for biomaterial-based polymer materials.

References

[1] R. J. Moon, A. Martini, J. Nairn, J. Youngblood, A. Martini, and J. Nairn 2011 *Chem Soc Rev*. **40** 3941-94
[2] M. Moniruzzaman and T. Ono 2012 Bioresour. Technol. 127 132–7
[3] M. George and C. Montemagno 2017 *Int. Ref. J. Eng. Sci.* **6** (5) 55–76 [Online]. Available: http://www.irjes.com/Papers/vol6-issue5/I6515576.pdf.
[4] A. H. Tayeb, E. Amini, S. Ghasemi, and M. Tajvidi 2018 *Molecules* **23** (2684) 1–24
[5] M. A. Hubbe, O. J. Rojas, and L. A. Lucia 2015 *BioResources* **10** (3) 6095–6206 [Online]. Available: www.consumerreports.org.
[6] S. Mun, H. C. Kim, H. Ko, L. Zhai, J. W. Kim, and J. Kim 2017 *Sci. Technol. Adv. Mater*. **18** (1) 1–10
[7] M. A. Hubbe, A. Pizzi, H. Zhang, and R. Halis 2018 *BioResources* **13** (1) 2049–115
[8] H. Wei, K. Rodriguez, S. Renneckar, and P. J. Vikesland 2014 *Environ. Sci. Nano* **1** (4) 302–16,
[9] D. H. Camacho, S. R. A. E. C. Gerongay, and J. P. C. Macalinao 2013 *Cellulose Chem. Technol*., **47** (1-2) 125-32
[10] J. C. Courtenay, R. I. Sharma, and J. L. Scott 2018 *Molecules* **23** (3)
[11] N. Lin and A. Dufresne 2014 *Eur. Polym. J.* **59** 302–25
[12] H. Zhu, W. Luo, P.N. Ciesielski, Z. Fang, J.Y. Zhu, G. Henrikson, M.E., Himmel, L. Hu 2016 *Chem. Rev.* **116** (16) 9305–74
[13] T. C. Nirmale, B. B. Kale, and A. J. Varma 2017 *Int. J. Biol. Macromol*. **103** 1032–43
[14] J. C. Sta and D. H. Camacho 2019 *Mater. Chem. Phys*. **228** (February) 187–93
[15] K. H. Gardner and J. Blackwell 1974 *Biopolymers* **13** (10) 1975–2001
[16] M. C. Jarvis 2018 *Philos. Trans. R. Soc. A Math. Phys. Eng. Sci*. **376** (2112) 1–13

[17] D. Klemm, B. Heublein, H. P. Fink, and A. Bohn 2005 *Angew. Chemie - Int. Ed.* **44** (22) 3358–93
[18] D. Trache, M.H. Hussin, C.T. H. Chuin, S. Sabar, M.R. N. Fazita, O.F.A. Taiwo, T.M. Hassan, M.K.M. Haafiz 2016 *Int. J. Biol. Macromol.* **93** (June) 789–804
[19] D. Trache, K. Khimeche, A. Mezroua, and M. Benziane 2016 *J. Therm. Anal. Calorim.* **124** (3) 1485–96
[20] M. E. Fuller, C. Andaya, and K. Mcclay 2017 *J. Microbiol. Methods* **144** (October) 145–51
[21] S. M. L. Rosa, N. Rehman, M. I. G. De Miranda, S. M. B. Nachtigall, and C. I. D. Bica 2012 *Carbohydr. Polym.* **87** (2) 1131–38
[22] C. P. Azubuike and A. O. Okhamafe 2012 *Int. J. Recycl. Org. Waste Agric.* **1** (1)
[23] M. K. M. Haafiz, A. Hassan, Z. Zakaria, I. M. Inuwa, M. S. Islam, and M. Jawaid 2013 *Carbohydr. Polym.* **98** (1) 139–45
[24] Z. Xiang, W. Gao, L. Chen, W. Lan, and J. Y. Z. Troy 2016 *Cellulose* **23** (1) 493–503
[25] C. C. Beads, I. Rocha, Y. Hattori, M. Diniz, A. Mihrayan, M. Stromme, J. Lindh 2018 *Langmuir* **34** (August) 11121–25
[26] J. I. Moran, V. A. Alvarez, V. P. Cyras, and A. Vasquez 2008 *Cellulose* **15** 149–59
[27] A. M. Adel and N. A. El-Shinnawy 2012 *Int. J. Biol. Macromol.* **51** (5) 1091–102
[28] H. Yang, R. Yan, H. Chen, D. H. Lee, and C. Zheng 2007 *Fuel* **86** 1781–1788
[29] M. Z. Karim, Z. Z. Chowdhury, S. B. A. Hamid, and M. E. Ali 2014 *Materials (Basel)* **7** (10) 6982–99
[30] J. Shi and L. Jian 2012 *BioResources* **7** (3) 3463–75
[31] N. Keshavarzi, F.M. Rad, A. Mace, F. Ansari, F. Akhtar, U. Nilsson, L. Berglund, L. Bergstrom 2015 *ACS Appl. Mater. Interfaces* 7 (26) 14254-62
[32] S. Zhou, L. Nyholm, M. Strømme, and Z. Wang *2019 Acc. Chem. Res.* **52** (8) 2232–2243
[33] C. Zhou and Q. Wu 2012 Recent Development in Applications of Cellulose Nanocrystals for Advanced Polymer-Based Nanocomposites by Novel Fabrication Strategies Nanocrystals - Synthesis, Characterization and Applications chapter 6 pp 103–120
[34] A. Mihranyan, A. Piñas, R. Karmhag, M. Strømme, and R. Ek 2004 *International journal of pharmaceutics* **269** 433–42
[35] S. Kalia, A. Dufresne, B.M. Cherian, B.S. Kaith, L. Averous, J.Njuguna, E. Nassiopoulos 2011 *Int. J. Polym. Sci.* **2011** 2-35
[36] M. Camacho, Y.R.C. Urena, M. Lopretti, L.B. Carballo, G. Moreno, B. Alfaro, J. R.V. Baudrit 2017 *J. Renew. Mater.* **5** (3–4) 271–9
[37] K. G. Bogolitsyn, P. A. Kaplitsin, A. E. Parshina, A. S. Druzhinina, and D. V Ovchinnikov 2017 *Russian Journal of Applied Chemistry* **90** (11)
[38] E. Abraham, B. Deepa, L.A. Pothan, M. Jacob, S. Thomas, U. Cvelbar, R. Anandjiwala 2011 *Carbohydr. Polym.* **86** (4) 1468–75
[39] J. H. Kim, B.S. Shim, H.S. Kim, Y.J. Lee, S..K. Min, D. Jang, Z. Abas, J.Kim 2015 *Int. J. Precis. Eng. Manuf. - Green Technol.* **2** (2) 197–213
[40] O. Nechyporchuk, M. N. Belgacem, and J. Bras 2016 *Ind. Crops Prod.* **93** 2–25
[41] P. Phanthong, P. Reubroycharoen, X. Hao, and G. Xu 2018 *Carbon Resour. Convers.* **1** (1) 32–43
[42] R. Xiong, X. Zhang, D. Tian, Z. Zhou, and C. Lu 2012 *Cellulose* **19** (4) 1189–98
[43] H. P. S. A. Khalil, Y. Davoudpour, N. Islam, M. Asniza, K. Sudesh, R. Dungani, M. Jawaid 2014 *Carbohydr. Polym.* **99** 649–65
[44] Y. Chen, Q. Wu, B. Huang, M. Huang, and X. Ai 2015 *BioResources* **10** (1) 684–96
[45] D. Zheng, Y. Zhang, Y. Guo, J. Yue 2019 *Polymers* **11** (1130) 1-14
[46] I. M. A. G. W. I Gusti Ngurah Jemmy Anton Prasetia, Shelia Deviana, Trisna Damayanti, Angga Cahyadi 2018 *J. Farm. sains dan komunitas* **15** (2) 68–71
[47] T. Isogai, M. Yanagisawa, and A. Isogai 2008 *Cellulose* **15** (6) 815–23
[48] R. Gupta and Y. Y. Lee 2010 *Biotechnol. Prog.* **26** (4) 1180–86

[49] J. Xu, J. J. Cheng, R. R. Sharma-Shivappa, and J. C. Burns 2010 *Energy and Fuels* **24** (3) 2113–19
[50] H. Kargarzadeh, I. Ahmad, I. Abdullah, A. Dufresne, S. Y. Zainudin, and R. M. Sheltami 2012 *Cellulose* **19** (3) 855–66
[51] V. Hospodarova, E. Singovszka, and N. Stevulova 2018 *Am. J. Anal. Chem*. **9** 303–10
[52] H. Dai, S. Ou, Y. Huang, and H. Huang 2018 *Cellulose* **25** (3) 1743–56
[53] D. Jagadeesh, D. Jeevan Prasad Reddy, and A. Varada Rajulu 2011 *J. Polym. Environ*. **19** (1) 248–53
[54] Q. He, Q. Wang, H.Zhou, D. Ren, Y. He, H. Cong, L. Wu 2018 *Cellulose* **25** (10) 5523–33